Structural Damage Assessments from Ikonos Data Using Change Detection, Object-Oriented Segmentation, and Classification Techniques

D.H.A. Al-Khudhairy, I. Caravaggi, and S. Giada

Abstract

Recent improvements in the spatial resolution of commercial satellite imagery make it possible to apply very high-resolution (VHR) satellite data for assessing structural damage in the aftermath of humanitarian crises, such as, armed conflicts. Visual interpretation of pre- and post-crisis very high-resolution satellite imagery is the most straightforward method for discriminating structural damage and assessing its extent. However, the feasibility of using visual interpretation alone diminishes in the cases of large and dense urban settlements and spatial resolutions in the range of 2 m to 3 meters and larger. Visual interpretation can be further complicated at spatial resolutions greater than 1 m if accompanied by shadow formation and differences in sensor and solar conditions between the pre- and post-conflict images.

In this study, we address these problems through investigating the use of traditional change techniques, namely, image differencing and principle component analysis, with an object-oriented image classification software, e-Cognition. Pre-conflict Ikonos (2 m resolution) images of Jenin in the Palestinian territories and Brest (1 m resolution) in FYROM were classified using the e-Cognition software. Thereafter, the pre-conflict classification was used to guide the classification, using e-Cognition, of the pixel-based change detection analysis. The second part of the study examines the feasibility of using mathematical morphological operators to automatically identify likely structurally damaged zones in dense urban settings. The overall results are promising and show that object-oriented segmentation and classification systems facilitate the interpretation of change detection results derived from very high-resolution (1 m and 2 m) commercial satellite data. The results show that object-oriented classification techniques enhance quantitative analysis of traditional pixel-based change detection applied to very high-resolution satellite data and facilitate the interpretation of changes in urban features. Finally, the results suggest that mathematical morphological methods are a potential new avenue for automatically extracting likely damaged zones from very high-resolution satellite imagery in the aftermath of disasters.

Introduction

Very high-resolution (VHR) (i.e., 2 m or smaller) space-borne remote sensing could play a unique role supplementing information from other sources in the response, relief, and reconstruction phases of disasters such as earthquakes and armed conflicts. However, current satellite remote sensing does not play a major operational role during these three phases. There are several reasons why this is the case including climatic related aspects (cloud-cover restrictions in the case of optical satellite imagery), high cost of very high-resolution satellite data, time required between when satellite images are acquired and delivered until the answer is given for a specific disaster, spatial resolution (structural damage to buildings cannot be easily distinguished in medium and medium to high-resolution satellite imagery), temporal resolution (the ability to image a damaged region within a sufficient time to effectively impact disaster response), poor understanding by the humanitarian community of space-based support, as well as, technical aspects (relatively high level of specialist interpretation traditionally needed for processing and analysing satellite images), and shutter control in areas of conflict.

The most widely used satellite sensors for civilian applications have been optical sensors on board the Landsat Thematic Mapper (30 meter resolution), SPOT multi-spectral and panchromatic (20 meter and 10 meter resolution, respectively), and IRS-1D satellites (6 meter resolution). The spatial resolution of Landsat, SPOT and combined Landsat and IRS-1D is too coarse for performing detailed mapping (e.g., residences, infrastructure, and water sites in refugee camps) and reliable disaster damage assessment due to the small size of damaged structures in relation to the image pixel size. In addition, the temporal resolution of Landsat Thematic Mapper, SPOT and IRS-1D sensors (16, 26, and 24 days, respectively), particularly in the presence of cloud cover at the time of the disaster, limits the applicability of such medium and medium to high resolution sensors for post-disaster damage assessment.

The improvement in the temporal (1 to 3 days and 1 to 5 days for optical sensors on board Ikonos-2 and Quickbird satellites, respectively, depending on latitude) and spatial resolution of very high-resolution optical imagery such as Ikonos-2 (1 m resolution in the panchromatic mode and 4 m in multi-spectral bands) and Quickbird (0.61 m resolution in the panchromatic mode and 2.8 m in multi-spectral bands) for civilian applications, opens a new era for humanitarian relief operations. At these very high-resolutions, the amount

Joint Research Centre, Commission of the European Communities, Ispra 21020 (VA), Italy (delilah.al-khudhairy@cec.eu.int).

Photogrammetric Engineering & Remote Sensing
Vol. 71, No. 7, July 2005, pp. 825–837.

0099-1112/05/7107–0825/$3.00/0

of detail that can be detected increases by a factor of 100 when the resolution improves from 10 m to 1 m, so that individual buildings, houses and tents can be recognised in a VHR satellite image. Although there have been several applications of synthetic aperture radar (SAR) for post-earthquake building damage detection (Matsouka & Yamazaki, 2002 and 2003), there have been very few studies examining the applicability of very high-resolution optical data for estimating post-disaster structural damage (Mitomi *et al.*, 2002, Chiroiu *et al.*, 2001, Saito & Spence, in press). The major disadvantage of current SAR sensors, in comparison to 2 m or better VHR optical data, for damage assessment in urban environments, include insufficient spatial resolution and inadequacy of C-band wavelength characteristic of current space-based commercial SAR sensors (e.g., ERS-2 and RADARSAT-1) in comparison to L-band SAR systems for change detection due to rigid constraints on interferometric baseline and de-correlation due to vegetation. Other limitations that are related to stringent response requirements in earthquake and conflict disaster management include the insufficient availability of suitable pairs of SAR interferometry with suitable, short baselines.

However, although the reduction of the satellite image pixel size as a result of the availability of VHR satellite data has facilitated the recognition of individual objects such as houses, it poses a challenge to classical pixel-based change detection and image classification methods. Post-classification and pre-classification pixel-based change detection methods (Lunetta and Elvidge, 1998) have been applied for environmental monitoring (Lunetta *et al.*, 1998, Mücher *et al.*, 2000), agricultural surveys (Bruzzone and Serpuco, 1997), and urban studies (Li *et al.*, 1998, Nielsen *et al.*, 1998; Stow *et al.*, 2001). The post-classification comparison approach is the simplest change detection method and involves the analysis of spectral differences between two independently classified image dates to identify areas of change. The areas of change are thereafter directly extracted through a comparison of the classification results. The approach's main disadvantage is the high dependency of the change detection results on the individual classification accuracy. On the other hand, the pre-classification approach uses a single analysis of a combined data set of two or more dates to identify areas of change. The approach is based on pixel-wise operations or scene-wise and pixel-wise operations and comprises various techniques including composite analysis, image differencing, and principal components analysis (PCA). Algorithms usually have to be applied to the change detection analysis to distinguish between changed and unchanged pixels and to classify them (Lunetta and Elvidge, 1998). One of the main difficulties of change analysis techniques is related to the laborious procedure of isolating and classifying the changes.

Traditional pixel-based classification approaches have been widely used to characterize and discriminate between different types of image features in both classification and change detection applications involving agricultural, forest, and environmental monitoring. These methods are based on the concept that semantic information is represented in single pixels and are well suited for non-complex image scenes (e.g., spectrally homogeneous object classes). However, these methods have produced unsatisfactory results in the case of applications involving the characterisation of man-made structures and other heterogeneous features in urban environments (Haala and Brenner,1999). The main reason being that urban objects are distinguished better through their spatial (i.e., texture, form, area) rather than spectral reflectance properties (Zhang, 1999). In addition, traditional pixel-based classification methods cannot differentiate easily between object features that display high spectral overlap, such as, building roofs from pavements that are constructed using similar material (Kiema, 2002). Furthermore, in applications where VHR satellite imagery is used, it is necessary to expand the object feature base to include spatial characteristics in addition to spectral ones. Object-oriented segmentation and classification approaches offer possibilities to overcome these problems. These methods take into account knowledge of neighbourhood pixels when seeking to determine the most appropriate class for a pixel. They tend to develop a thematic map that is consistent both spectrally and spatially. However, the degree to which adjacent pixels are strongly correlated will depend on the spatial resolution of the satellite sensor and the scale of the image features. For example, adjacent pixels over agricultural land will be strongly correlated, whereas for the same sensor, adjacent pixels in a busier urban region would not show strong correlation. Object-oriented methods are generally based on the concept that important semantic information is not represented in single pixels alone but in meaningful image objects and their mutual relations (i.e., context).

In this paper, traditional change detection and two types of object-oriented approaches, a multi-resolution segmentation method followed by a supervised fuzzy logic classification (carried out with the commercial software eCognition (Definiens, 2001), and mathematical morphology (Soile, 2003) are applied to 1 m and 2 m resolution Ikonos satellite data to identify post-conflict damaged structures in two study areas: the Jenin refugee camp and the Former Yugoslav Republic of Macedonia (FYROM). The paper addresses two main problems associated with using VHR satellite to identify post-conflict structural damage: limitations of applying traditional change detection methods and interpretation of change analysis. The study first investigates the effectiveness of traditional change detection methods, image differencing and principal component analysis, in discriminating change pixels representing likely structurally damaged zones. Second, it investigates the ability of commercial object-oriented software such as eCognition, to interpret change detection analysis carried out with very high-resolution commercial satellite data. The final part of the study examines the feasibility of using a mathematical morphological technique implemented in the commercial software SDC (2001) to automatically identify likely structurally damaged zones in the Jenin case study. The results are promising and show that commercial object-oriented systems facilitate the interpretation of change detection results derived from very high resolution (1 m and 2 m) commercial satellite data. The results also indicate that change detection analysis based on relatively lower resolution satellite imagery (2 m) supplemented with object-oriented classification of change images could be used to discriminate likely structurally damaged zones. The results also show that mathematical morphological methods could be applied to automatically identify likely damaged zones in the aftermath of disasters.

Change Detection Methods

Pre-classification Change Detection

Image differencing is mathematically the simplest of the pre-classification change detection approaches, and it involves processing two multi-spectral images acquired at two different dates to generate a new image. The uni-variate image differencing method generates the difference image by subtracting, pixel by pixel, a single spectral band of the two multi-spectral images under analysis. The choice of the

spectral band depends on the specific type of change to be detected (Bruzzone and Prieto, 2000).

The PCA method transforms multi-variate data sets comprising inter-correlated variables into a data set consisting of variables that are uncorrelated linear combinations of the original variables (Ingebritsen and Lyon, 1985). The transformed variables are known as principle components (PC). The method entails superimposing two multi-date n-band image scenes to produce a single $2n$-band image. One of the advantages of the PCA method is that it can incorporate multi-temporal multiple bands of data for change detection. The first PCs tend to represent variation associated with unchanged features and overall image noise (e.g., atmospheric and seasonal variation, while the third and later PCs are usually of more relevance for identifying changed areas (Hayes and Sader, 1999). The next step is to identify which bands account for the largest amount of variance and which should be thereafter subjected to further analysis such as image classification. A variant of the PCA method is the standardized PCA method, which is based on the correlation matrix that is derived from the covariance matrix. The standardized PCA is intended to have additional advantages over the un-standardized PCA method such as improved interpretability, isolation of seasonal and surface illumination effects, as well as, variability due to noise.

The discrimination of change and no-change pixels from the change analysis can be analyzed using the classical thresholding method. Threshold levels are usually selected quantitatively according to empirical strategies or manual trial-and-error procedures (Bruzzone and Prieto, 2000). The most widely-used approach is based on the assumption that few changes occur in a given area. According to the assumption, pixels having values significantly different from the mean of the density function of the difference or the PCA image are labelled as changed. This concept assumes that if some changes have occurred between the multiple images, and the changes represent a small percentage of the total number of pixels of the scene, then the "change" pixels would lie in the tails, while the "unchanged pixels" would be grouped around the mean of the histogram of the change detection image (Figure 1). Usually the decision threshold is fixed at $n\sigma$ from the mean value of the change image where n is a number derived by trial-and-error and σ is the standard deviation of the density function of the pixel values in the change image. Generally, the following rules are applied:

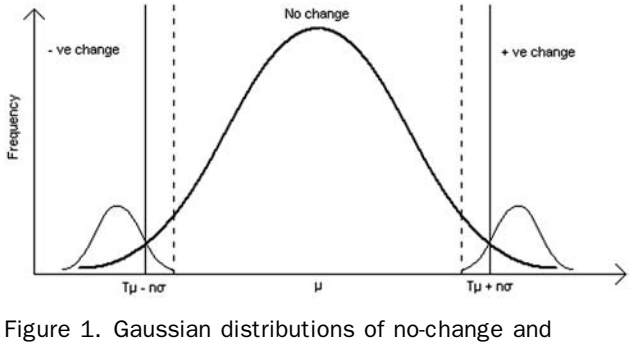

Figure 1. Gaussian distributions of no-change and positive and negative change pixels: μ represents the mean of the histogram of the change image, σ is the standard deviation of the density function of the pixels value in the change image, and n is the multiple of the standard deviation threshold.

"-ve change" if minimum value $<$ pixel value $<\mu - n\sigma$

"no change" if $\mu - n\sigma <$ pixel value $< \mu + n\sigma$

"+ve change" if $\mu + n\sigma <$ pixel value $<$ maximum value

where μ is the mean.

Once the threshold is determined, the change image can be classified to produce a labeled change product. An innovative approach to interpret and classify change results is to apply the objected-oriented image classification software such as eCognition (Niemeyer and Canty, 2001) to the spectral change data.

Object-oriented Image Segmentation and Classification with eCognition

eCognition is an object-oriented image analysis software package that brings together multi-resolution segmentation and knowledge-based analysis methods (Definiens, 2001). The image analysis process with eCognition comprises two main steps: segmentation and classification.

Normal segmentation entails grouping image elements according to shape and spectral homogeneity. eCognition's segmentation algorithm is based on the bottom-up region-merging technique (Definiens, 2001). The method starts at an arbitrary point in the image with one-pixel objects, and in a number of segmentation steps, the pixel objects are enlarged to bigger pixel groups (segments) until a certain heterogeneity value (scale parameter) is reached. The larger the scale parameter, the larger the image segments. These segments are optimized using two other homogeneity criteria: shape and color. The product is a hierarchical network of image objects wherein fine objects are sub-objects of courser image structures. Thereafter, relations can be defined between image objects since each object knows its context, its neighborhood, and its sub-objects. In a second step, the defined local context information can thereafter be used together with additional semantic information for classification.

A special type of segmentation, knowledge-based, is also offered in eCognition. Knowledge-based segmentation allows the use of an already made classification as additional information for the merging of objects. Segments of one class can be merged on the same level or on a higher level than the one used for constructing the segments.

eCognition's knowledge-based approach offers two types of classification methods to classify objects into information categories: nearest neighbor and fuzzy membership functions. While the nearest neighbor classifier describes the classes to be identified through sample objects for each class defined by the user, fuzzy membership functions describe intervals of feature characteristics wherein objects belong or do not belong to a certain class by a certain degree. A class is thereafter described by combining one or more class descriptors by means of either fuzzy-logic operators or inheritance, or a combination of both. The entire process of image analysis with eCognition can be summarized as follows (Definiens, 2001):

- applying the multi-resolution segmentation to create a hierarchical network of image objects,
- classifying the derived objects by their physical properties,
- describing semantic relationships of the network's objects in terms of neighborhood relationships or being a sub- or super-object,
- aggregating the classified objects into contiguous semantic groups which can be used thereafter in the classification-based segmentation. The derived segments can also thereafter be exported and analysis in a geographic information system (GIS).

While the first two steps are mandatory when analyzing images with eCognition, the last two steps are advisable to

improve the classification and to export the classified groups for further analysis in a GIS.

Object-oriented Image Segmentation and Classification with Mathematical Morphology

Mathematical morphology dates back to the study of porous media in the sixties, and evolved only recently to a recognized and mature discipline (Matheron and Serra, 1967). Soile (2003) defines mathematical morphology as a collection of operators based on set theory for the analysis of spatial structures. Mathematical morphology is also recognised as a powerful tool for image analysis and enhancement. Soile and Pesaresi (2002) and Soile (1996) have demonstrated the effectiveness of using mathematical morphology to extract structural information from optical satellite data.

The mathematical morphology approach to image analysis comprises two broad steps: segmentation and classification. The mathematical morphology approach to image segmentation combines region growing and edge growing techniques. The method groups the image pixels around the regional minima of the image, and the boundaries of adjacent groupings are precisely located along the crest lines of the gradient image. The segmentation is known as the watershed transformation and can partition the image into meaningful objects. Mathematical morphology can also be used for classification purposes. The watershed-based clustering based on applying non-parametric methods for finding clusters in multi-variate histograms is suited to both supervised and unsupervised classification approaches. However, multi-channel images cannot be directly processed by morphological operators. Soile (2003) applies morphological clustering in a feature space to the classification of multi-spectral images. The disadvantage of the technique is that it can only handle a maximum of three channels for practical applications. An alternative solution is to process each channel separately as a greyscale image. This is referred to as marginal ordering (Barnett, 1976) and is the approach used in this paper. The morphological tool used in this study is the SDC toolbox (SDC, 2001) which is based on MATLAB. The tool is a powerful collection of the latest morphological tools that can be applied to image segmentation, non-linear filtering, pattern recognition, and image analysis.

Most mathematical morphological operations are based on simple expanding and shrinking operations, namely erosion which shrinks an image object and dilation which expands it. Other morphological operators include opening, closing, and filtering. The neighborhood used for a given morphological operator is known as the structuring element (SE) whose shape is usually chosen according to *a priori* knowledge about the geometry of the relevant and irrelevant image structures. For example, linear structuring elements are suitable for extracting linear objects. Some of the basic morphological operators used in this study are described as follows.

The eroded value at a given pixel x is the minimum value of the image in the window defined by the SE when its origin is at x:

$$e_B(f)(x) = \min\{f(y): y \in (B + x) \cap E\} \quad (1)$$

where $E = \{1,2, \ldots ..,H\} \times (1,2, \ldots ..,W\}$ and H and W are, respectively, the number of rows and columns of the image f.

The dilated value at a given pixel x is the maximum value of the image in the window defined by the SE when its origin is at x:

$$\delta_B(f)(x) = \max\{f(y): y \in (\check{B} + x) \cap E\} \quad (2)$$

where $E = \{1,2, \ldots ..,H\} \times (1,2, \ldots ..,W\}$ and H and W are, respectively, the number of rows and columns of the image f. $\check{B}$ is the transposition set of B and correspond to its symmetric set with respect to its origin.

The opening operator smoothes a contour in an image, closing tends to narrow sections of contours, and filtering is used for edge enhancement and extraction or suppression of selected image structures. The opening of an image f by a structuring element B is defined as the erosion of f by B followed by the dilation with the transposed SE of B:

$$\gamma_B(f) = \delta_{\check{B}}[e_B(f)] \quad (3)$$

Although the opening is defined in terms of erosion and dilation, it possess a geometric definition in terms of SE fit using the question already introduced for the erosions: "Does the SE fit the set?". Each time the answer is affirmative, the whole SE must be kept. Therefore, the opened set is the union of all SEs fitting the set:

$$\gamma_B(f) = \cup\{B/B \subseteq X\} \quad (4)$$

Closing tends to recover the initial shape of the image structures that have been dilated. This is achieved by eroding the dilated image:

$$\phi_B(f) = e_{\check{B}}[\delta_B(f)] \quad (5)$$

Using set theory, we can define the following question for a closing: "Does the SE fit the background of the set?", if yes all points of the SE belong to the complement of the closing of the set:

$$\gamma_B(f) = \cap\{B^c/X \subseteq B^c\} \quad (6)$$

Soile (2003) provides a more complete description of the morphological operators used in this study as well as morphological operators in general.

Study Areas and Materials

Former Yugoslav Republic of Macedonia (FYROM)

The International Management Group (IMG) was contracted by the European Commission at the end of the conflict in August 2001 to carry out a one month field-based damage assessment in 11 municipalities in the Northern and Western parts of the Former Yugoslav Republic of Macedonia (FYROM) during September and October 2001 (IMG, 2001). The aim of the IMG assessment was to estimate the scale and cost of urgent repairs of houses and relevant infrastructure to facilitate the return of refugees and homeless people to their homes before the beginning of winter 2001. Although IMG was able to identify four types of structural damage classes, ranging from low to highly severe damage, in 26 accessible villages, they were unable to conduct ground-based surveys in 28 villages because they were inaccessible for several reasons including general security, high presence of unexploded objects, and mined roads.

The available satellite images for the Brest study site in FYROM consisted of two, cloud-free, pan-sharpened images, acquired on 12 May 2000 and 01 May 2001. The look and sun angles of the pre- and post- images are 87.26° and 60.95°, and 78.33° and 59.6°, respectively. The 1 m resolution panchromatic (0.45–0.90 μm) and 4 m resolution multispectral bands (0.45–0.52, 0.52–0.60, 0.63–0.69, 0.76–0.90 μm) were merged, using principle component analysis (PCA), to produce new images with the spatial resolution of the panchromatic band and the spectral resolution of the multispectral bands. While guaranteeing that each band is sharpened, the PCA method maintains the original bit range, number of bands as well as the spectral values.

Jenin-West Bank

The Jenin refugee camp is located North of the West Bank and is mainly composed of buildings of two to three storeys, in concrete and brick, of which approximately 200 were partially or totally damaged during the incursion in April 2002 (Chandler, 2002; UN, 2002). In the aftermath of the incursion, although agencies were permitted to enter the camp under military escort, their access was restricted to certain areas only, and was further constrained by presence of large quantities of unexploded ordnance, including booby traps. The agencies aborted their efforts shortly after entering the camp with the result that no ground-based damage verification was carried out at that time.

The available satellite images for the study site consisted of two 2 m pan-sharpened images, one was acquired on 24 December 2001 and the other on 07 May 2002. The look and sun angles of the pre- and post- images are 61.09° and 32.36°, and 50.43° and 66.28°, respectively. The 1 m resolution panchromatic (0.45–0.90 μm) and 4 m resolution multi-spectral bands (0.45–0.52, 0.52–0.60, 0.63–0.69, 0.76–0.90 μm) were merged, using principle component analysis (PCA), to produce new images with the spatial resolution of the panchromatic band and the spectral resolution of the multi-spectral bands.

Methodology

Overview

Three damage detection approaches were investigated in this study (Figure 2). In the first approach, four different types of temporal pixel-based change detection methods were compared in the FYROM and Jenin study sites: standardized and un-standardized principal component analysis and calibrated (radiometrically corrected) and un-calibrated (radiometrically uncorrected) image differencing. The change results were thereafter interpreted and classified using the object-oriented image segmentation and classification software, eCognition. The second and third approaches entailed applying the eCognition and mathematical morphology SDC software packages directly to the post-disaster images in the FYROM and Jenin study sites, respectively.

The images in both study sites were geometrically corrected with the Georis® software (Acri, 2002) using a first order polynomial model and the nearest neighbor re-sampling method. Georis® is specially designed for image rectification and georeferencing and performs better than other traditional software since it applies both local (related only to the neighboring pixels) and global (related to the whole image) models. A digital elevation model (DEM) of 25 m grid cell resolution and 1 meter vertical accuracy of both study areas was also used to perform the registration. Registration was performed with and without the DEM. However, since the difference in the results was insignificant, we selected the images registered using the DEM for the change detection analysis. Mis-registration errors in the study sites were found to vary from a total root mean square error (RMSE) of 0.91 m in the case of FYROM to 5.7 m in the case of Jenin. The average mis-registration errors in Jenin and Brest are 4.48 m and 0.75 m, respectively.

Approximate radiometric rectification of the images in both study sites for the calibrated image differencing test was carried out with ENVI's tool "Empirical Line Calibration" (Research Systems, Inc., 1999). The tool uses spectral data collected in both images as radiometric control sets. The data were collected for the same land cover types. ENVI's tool "Empirical Line Calibration" forces spectral data to match selected field reflectance spectra. A linear regression (Lunetta and Elvidge, 1998) was used to equate each band in the reference image to the corresponding one in the second image. The radiance spectrum for each control set is extracted from the image and then mapped to the actual reflectance using linear regression techniques.

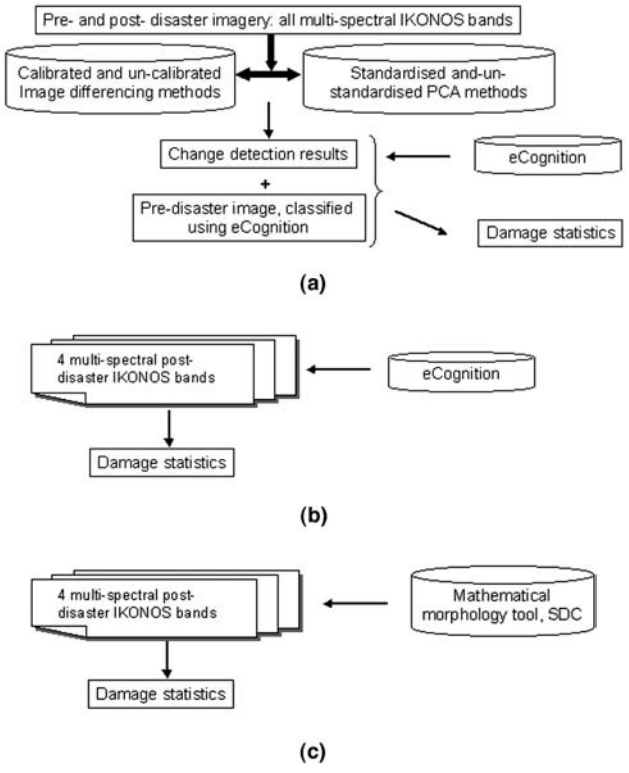

Figure 2. Flowchart of building damage detection methods applied to the study sites Jenin and Brest. (a) Approach 1 applied to Jenin and Brest (FYROM): building damage identification based on application of eCognition to results of change detection methods and classified pre-disaster imagery; (b) Approach 2 applied to Brest (FYROM), building damage identification based on application of eCognition to post-disaster imagery; (c) Approach 3 applied to Jenin: building damage identification based on application of mathematical morphology operations to post-disaster imagery.

Visual Interpretation

A visual comparison of pre- and post-conflict satellite images shows that only severe structural damage, such as, severely (total collapse of roof and only outer and inner walls remaining such as in the FYROM case study) or completely damaged (reduced to rubble), houses and buildings are recognizable (e.g., Jenin study site). The visual comparison showed that it was relatively more difficult to distinguish individual houses and buildings in dense urban settings with 2 m spatial resolution satellite data. These difficulties arise mainly due to difference in height between adjacent houses or buildings, and shadow of three story structures partially obscuring adjacent lower buildings or houses. On the other hand, individual built-up structures were easily recognizable with 1 m resolution data. In both study sites, the number and location of damaged houses and buildings were recorded and digitized through visual comparison of pre- and post-conflict images. These were

used to validate the three-change detection approaches applied in this study.

Change Detection and Object-oriented Change Classification of Change Images

Four different types of temporal change detection methods were compared: standardized and unstandardized principal component analysis, and calibrated (radiometrically corrected) and un-calibrated (radiometrically uncorrected) image differencing. In their paper (Al Khudhairy *et al.*, 2003), the authors show that areas of structural change can be detected in the second PC and the higher ones (PCs 6 and 8). The change detection results were thereafter interpreted and classified using the object-oriented image segmentation and classification software, eCognition (Definiens, 2001).

The eCognition software was first applied to the pre-disaster, baseline images of both study sites in order to produce an object oriented classification comprising four classes: paved surface, vegetation, built-up structures (e.g., houses and buildings), and shadow. Table 1 summarizes the segmentation parameters used to provide optimal classification results of the pre-disaster images for both study sites. Generally, the lower segmentation levels were used to classify individual houses or buildings and roads, whereas the higher levels were used to classify larger objects in the study sites such as cultivated and uncultivated fields referred to herein as vegetation. In FYROM, the image segments were classified using several fuzzy-membership functions for area, brightness, length/width ratio, standard deviations of spectral band values, distance between neighboring objects, and mean difference to scene (Al Khudhairy *et al.*, 2003). On the other hand, a mixed approach was applied in the Jenin study site. The approach entailed applying fuzzy membership functions to classify built-up structures and roads, and standard nearest neighbour classifiers to classify shadow and vegetation objects due to their highly irregular shape. Plate 1 shows the results of the classification of the pre-disaster images of both study sites, which were used thereafter as input thematic layers in the segmentation and classification of the change data.

A knowledge-based, bottom up, region-merging segmentation, approach was applied using eCognition in order to extract meaningful image objects from the change input data (image difference bands and principal components). The knowledge-based segmentation approach makes use of pre-disaster classifications as additional information to guide the merging of objects during the segmentation process and their classification thereafter. Tables 2 and 3 summarize the segmentation parameters established on the basis of contextual information (scale, color, and form), the change bands or principal components, and the produced segments or objects capturing the shape and size of individual buildings or houses in the study sites.

A three-step classification approach was applied to the image objects extracted in the final segmentation level in order to identify and label the structurally damaged zones. In the first classification step, Equations 1 through 3 were formulated in eCognition's fuzzy membership functions in order to discriminate between *change* and *no change* objects through extracting, in terms of standard deviations, three parent classes: *change* (positive and negative) and *no-change*. The positive and negative change classes each have three to four identical child classes depending on the study site: vegetation, paved surface, buildings and/or houses, and other man-made features. In the *no change* case, the image difference bands and the principal components range between the mean minus one standard deviations on the left border and the mean plus one standard deviations on the right border (Figure 1). In the *positive and negative change* cases, the image difference bands and the principal components have to be smaller or larger respectively than the mean, minus, or plus a multiple of the standard deviations on the left border (negative change) and the right border (positive change). In addition, relations were generated using eCognitions fuzzy membership function so that shadow objects were not classified as *change/no change* objects.

In the second step, the classified pre-disaster images are used as thematic input layers in eCognition to provide extra information to further refine the *change* classes to extract four main types of change that have occurred: vegetation, paved surfaces, buildings and/or houses, other man-made features.

In the third step, the final classification of damaged zones takes place in order to classify only *change* objects coinciding with buildings or houses as structurally damaged zones. The pre-disaster classified thematic layer determines which positive and negative change objects coincide with pre-disaster buildings or houses to minimize misclassifications. The result is a classified map showing likely damaged houses and/or buildings (Plates 2 and 3). The shadow class is not shown in the final classified image.

TABLE 1. PARAMETERS APPLIED FOR THE SEGMENTATION AND CLASSIFICATION OF THE PRE-DISASTER, BASELINE IMAGES OF THE JENIN AND FYROM (BREST) STUDY SITES

			Segmentation Parameters								
								Homogeneity Criterion			
			Ikonos-2 Bands Used							Shape Setting	
Study Site	Segmentation and Classification Level	Land Use Types	Red	Green	Blue	NIR	Scale Parameter	Colour	Shape	Smoothness	Compactness
Jenin	Level 1	Shadows	yes	yes	yes	yes	10	0.8	0.2	0.9	0.1
	Level 2	Houses/buildings	yes	yes	yes	yes	70	0.8	0.2	0.9	0.1
	Level 3	Vegetation, uncultivated land, and roads	yes	yes	yes	yes	90	0.8	0.2	0.9	0.1
FYROM	Level 1	All	yes	yes	yes	yes	10	0.7	0.3	0.9	0.1
	Level 2	Houses/buildings	yes	no	no	no	20	0.7	0.3	0.9	0.1
	Level 3	Vegetation, uncultivated land, and roads	yes	no	yes	yes	30	0.7	0.3	0.9	0.1

TABLE 2. SEGMENTATION PARAMETERS APPLIED IN THE IMAGE DIFFERENCING CHANGE ANALYSIS OF JENIN AND FYROM (BREST)

Study Site	Segmentation/ Classification Level	Change Detection Method	Segmentation Parameters: Ikonos-2 Bands Used: Red	Green	Blue	NIR	Scale Parameter	Mean Object Size	Homogeneity Criterion: Colour	Shape	Shape Setting: Smoothness	Compactness
Jenin	Level 1	Calibrated	yes	yes	yes	yes	10	7.4	0.8	0.2	0.5	0.5
	Level 2	image	yes	yes	yes	yes	15	12.3	0.8	0.2	0.5	0.5
	Level 3	differencing	yes	yes	yes	yes	20	19.5	0.8	0.2	0.5	0.5
	Level 1	Non calibrated	yes	yes	yes	Yes	10	10.1	0.8	0.2	0.5	0.5
	Level 2	image	yes	yes	yes	Yes	15	19.4	0.8	0.2	0.5	0.5
	Level 3	differencing	yes	yes	yes	Yes	20	31.7	0.8	0.2	0.5	0.5
FYROM	Level 1	Calibrated	yes	yes	no	no	10	9.92	0.8	0.2	0.9	0.1
	Level 2	image differencing	yes	yes	no	no	15	22.92	0.8	0.2	0.9	0.1
	Level 1	Non calibrated	yes	yes	no	no	10	11.62	0.8	0.2	0.9	0.1
	Level 2	image differencing	yes	yes	no	no	15	26.30	0.8	0.2	0.9	0.1

TABLE 3. SEGMENTATION PARAMETERS APPLIED IN THE PCA CHANGE ANALYSIS OF FYROM (BREST) AND JENIN

Study Site	Segmentation/ Classification Level	Change Detection Method	Segmentation Parameters: Scale Parameter	Mean Object Size	Homogeneity Criterion: Colour	Shape	Shape Setting: Smoothness	Compactness
Jenin	Level 1	Standardised PCA	10	19.5	0.8	0.2	0.5	0.5
	Level 2		15	38.9	0.8	0.2	0.5	0.5
	Level 1	Non Standardised PCA	10	20.9	0.8	0.2	0.5	0.5
	Level 2		15	40.7	0.8	0.2	0.5	0.5
FYROM	Level 1	Standardised PCA	10	16.87	0.8	0.2	0.9	0.1
	Level 2		15	43.8	0.8	0.2	0.9	0.1
	Level 1	Non Standardised PCA	10	15.68	0.8	0.2	0.9	0.1
	Level 2		15	49.19	0.8	0.2	0.9	0.1

Structural Damage Identification with eCognition

In the second approach, eCognition is applied directly to the post-disaster image of the FYROM study site. Table 4 summarizes the segmentation parameters established on the basis of contextual information (scale, color, and form), spectral bands, and the produced segments or objects capturing the complexity, in terms of land cover, of the input image data. Preference was given to spectral homogeneity as opposed to shape, in order to reduce the number of non-urban features misclassified as damaged or undamaged urban classes. However, this procedure was done at the expense of producing poorly-defined outlines of urban features. This procedure was acceptable given that the objective of the study was to assess the effectiveness of the method to identify and extract likely damaged houses and/or buildings. Next, each of the above segmentation levels were classified, using fuzzy rules, into several land-cover classes (including roads, vegetation, dark roofs, bright roofs, interior/outer walls of damaged houses, and shadow or ground separating these walls). Thereafter, a classification-based fusion was applied to levels 1 and 2 to merge the two following main types of image objects making up damaged and undamaged houses in order to represent them by individual meaningful image objects: dark roof in the shade and bright roof in the sun in the case of undamaged houses, and walls and shadow or ground separating the walls in the case of damaged houses (Plate 4). Thereafter, fuzzy rules using class related features (relation to features, length, area, brightness, length/width ratio, and standard deviations of spectral band values) were applied to produce the final classification of damaged houses shown in Plate 5 (show only roads, vegetation, uncultivated land, undamaged house, damage house).

Structural Damage Identification with Mathematical Morphology

A multi-level combined segmentation and classification approach was used to extract likely damage zones from the post-crisis Ikonos imagery acquired for the Jenin study site (Plate 6a). A marginal ordering approach was used whereby each of the four multi-spectral Ikonos bands is processed separately. An opening using a disk size structural element of a suitable size, followed by *reconstruction by dilation* and a *regional minimus* operation, was applied to each input band to isolate the crisis zone in the study site and to remove irrelevant image objects that do not contain the structural element. Successive *erosions* were applied to the intermediate output image to ensure that markers of adjacent objects are disconnected. The eroded sets are then used as seeds for *reconstruction by dilation* to further delete irrelevant image objects. The intermediate output is a binary image where the foreground pixels belong to the connected components with the highest spectral value in the matrix output from the *reconstruction by dilation* operation. Thereafter, *hit-or-miss* transformations were used to extract isolated, connected, very long thin image objects that are larger than the crisis zone, followed by *subtraction* and *reconstruction by dilation* to recover the original shape of

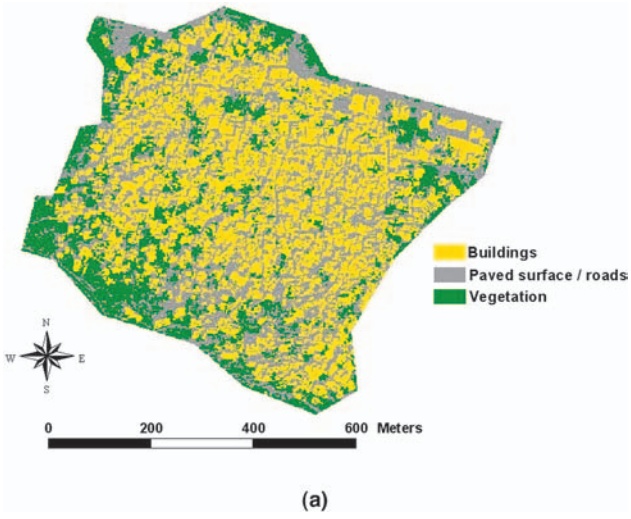

(a)

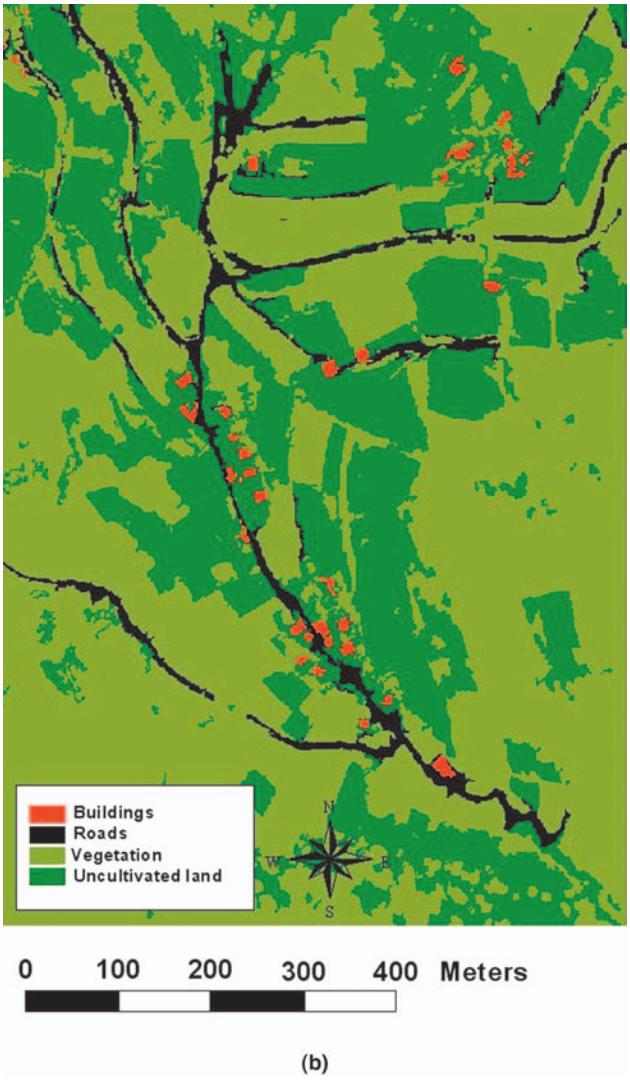

(b)

Plate 1. Classification of pre-disaster images of (a) Jenin and (b) Brest in FYROM study sites, using eCognition.

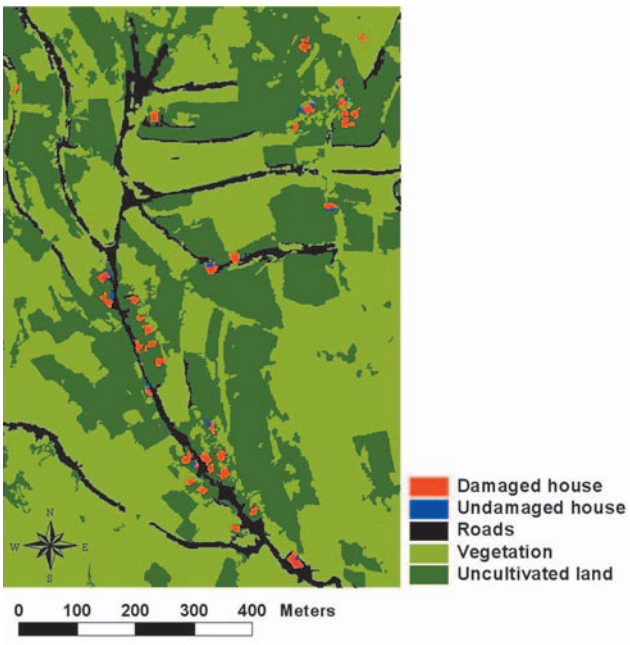

(a)

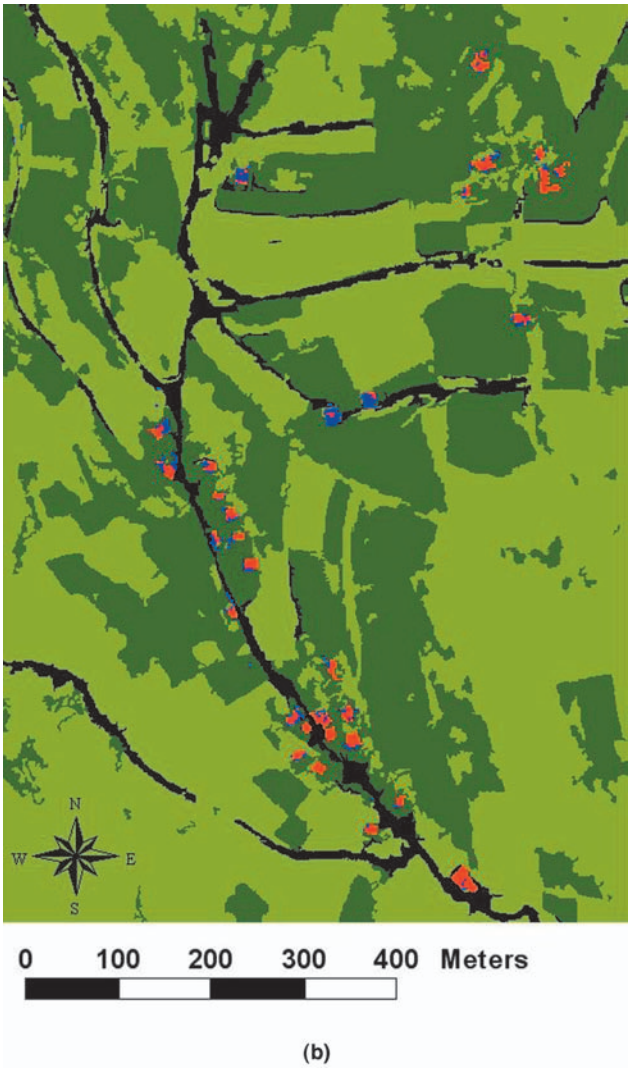

(b)

Plate 2. Classification of change images in FYROM (Brest) using eCognition: (a) Comparison of classifications based on standardised PCA and (b) calibrated image differencing.

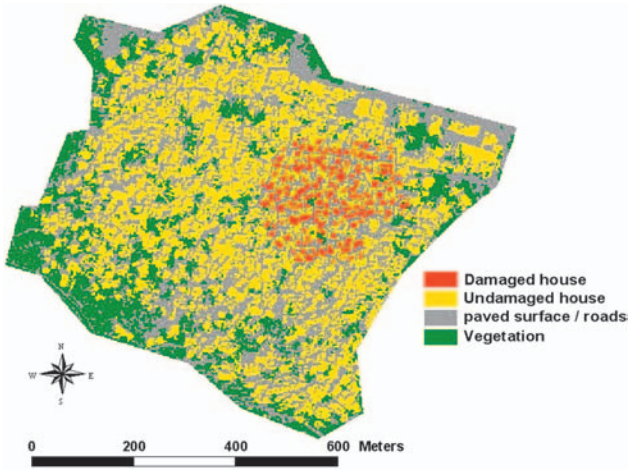

Plate 3. Classification of calibrated image differencing image in Jenin, using eCognition.

the crisis zone. Next, a dilation operation is applied to recover the original shape of the crisis zone. The intermittent results show that while the aforementioned approach can successfully extract the crisis zone in the near-infra-red (NIR) band, the remaining bands (red, green, and blue) contain additional irrelevant image objects. A *labelling* technique is next applied to the intermediate results obtained with the red, green, and red bands to isolate those irrelevant image objects through only extracting the area of interest. The final results of applying the approach described herein to the four bands, near-infra-red (NIR), blue, green and red are shown in Plate 6a.

The classification with mathematical morphology is next carried out by applying a series of operators to the blue band image (Plate 6b): bright features comprising built-up areas and roads are extracted by applying a *top-hat by opening* operator to the image, followed by thresholding to extract a mask for the relevant image objects. The road classification with mathematical morphology was based on importing a digitized road network as a large structuring element. The input road image is dilated and intersected with the bright image extracted in the aforementioned *top-hat by opening* operation to retrieve only the road network. The built-up area class is extracted by subtracting the road network from the bright zones matrix. The vegetation class is retrieved by negating the bright zone image extracted in the *top-hat by opening* operation and deleting from it very small isolated image objects. The final classification is achieved through combining these separately classified features (Plate 7).

Results and Analysis

The damage classification results of the three change detection approaches investigated in this study are compared to manually digitized damage maps of the two study sites in order to produce statistical information concerning the errors produced by these methods. The reference data for the manually digitized damage maps are pre- and post-conflict satellite scenes of FYROM (Brest) and Jenin. A detailed comparison is given in Tables 5 and 6. Table 5 shows the accuracy assessments, in terms of commission and omission errors, obtained for the first two methods: object-oriented classification, using eCognition, of change images, and automatic damage classification with eCognition. The values in the table represent the number of man-made structures correctly and incorrectly identified as damaged. Table 6 summarizes the accuracy, in terms of confusion error matrices, of the application of the third method, mathematical morphology to the Jenin study sites. All three methods were assessed for their ability to accurately discriminate and classify post-conflict damaged buildings and houses in the two study sites.

Table 5 shows that both standardized and non-standardized principle component analysis (PCA) approaches performed similarly to the calibrated and non-calibrated image differencing methods in the FYROM study site. On the hand, the table shows that the non-standardized PCA and non-calibrated image differencing method performed worse than standardized PCA and calibrated image differencing approaches in the two study sites. However, in both study sites, the calibrated image differencing method performed similarly to the standardized PCA. The difference in the accuracy errors of the four methods could be attributed to the notable difference in the density of the built-up areas in both study sites; Jenin has a much higher built-up area density than Brest. Second, the buildings in Jenin were found to vary in height resulting in the problem of shadows in the cases of closely situated buildings. The difference in errors can also be explained by the difference in the resolution of the satellite data used (1 m versus 2 m resolution) as well as in registration errors. With 2 m resolution satellite data, it is more difficult to separate individual buildings in densely built-up areas. In addition, the average mis-registration errors in Jenin (4.48 m) were notably greater than in Brest, FYROM (0.75 m).

Table 5 shows that the errors acquired in the case of the post-classification using eCognition method were similar to

TABLE 4. SEGMENTATION PARAMETERS APPLIED IN THE CLASSIFICATION OF THE POST-CONFLICT IMAGE OF FYROM (BREST)

Segmentation/ Classification Level	Feature Types	IKONOS-2 Bands Used (Yes or No)				Scale Parameter	Homogeneity Criteria			
									Shape Setting	
		R	B	G	NIR		Color	Shape	Smoothness	Compactness
1	Damaged houses (walls and shadow/ ground separating walls)	Y	N	Y	Y	15	0.7	0.3	0.9	0.1
2	Undamaged Houses (bright and dark roof)	Y	N	Y	Y	20	0.7	0.3	0.9	0.1
3	Vegetation*/roads	Y	N	N	Y	30	0.8	0.2	0.5	0.5

*Vegetation includes cultivated/uncultivated land and trees.

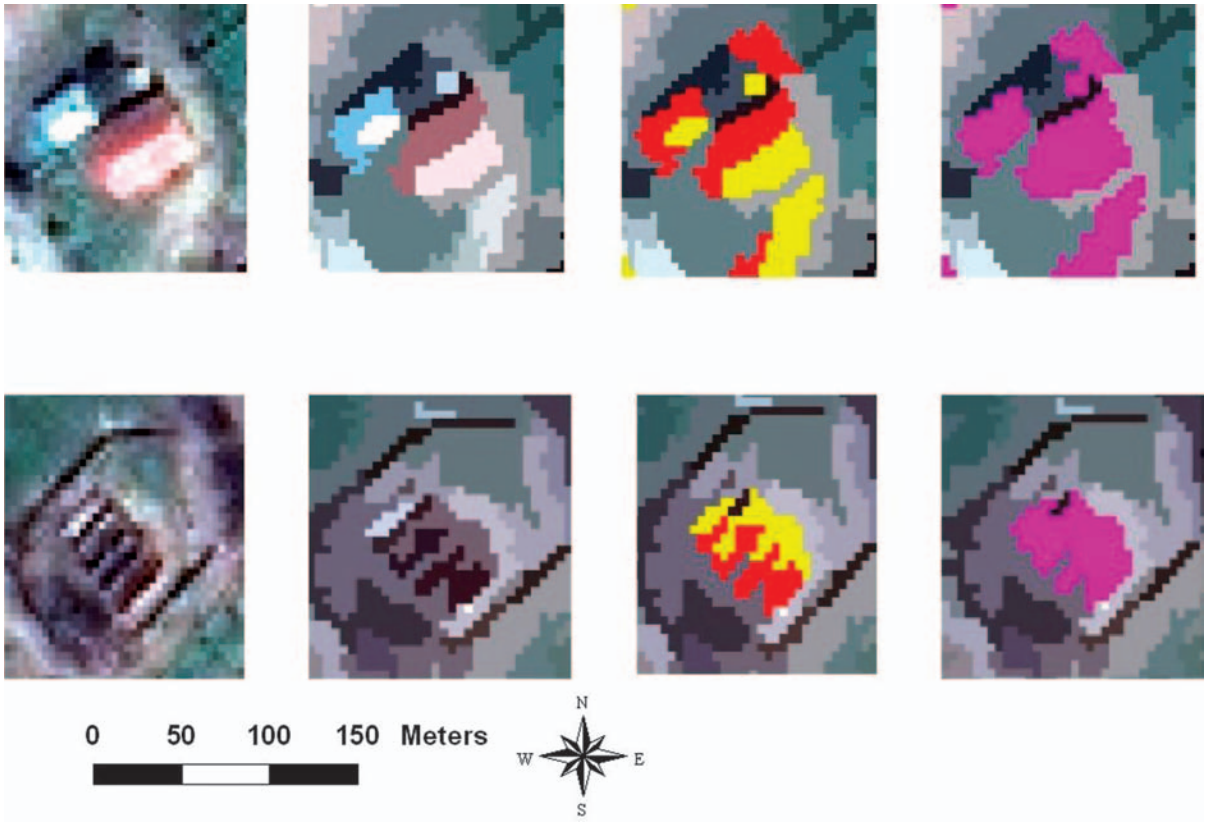

Plate 4. Four different stages of segmentation and classification when eCognition is applied directly to post-conflict images: undamaged structures (top) and damaged structures (bottom) in FYROM (Brest).

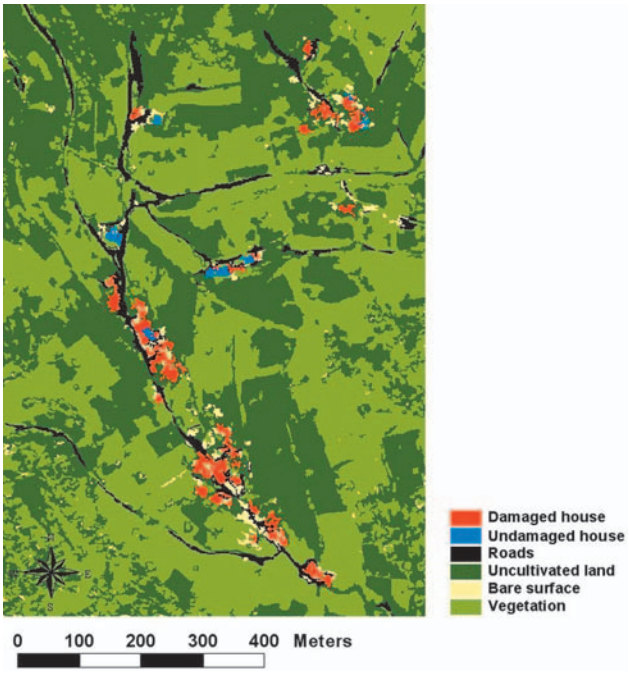

Plate 5. Results of object-oriented, using eCognition, classification of post-conflict image in FYROM (Brest).

the ones obtained for the PCA and image differencing methods applied in the FYROM (Brest) study site. Moreover, although the post-classification method yields no omission errors with respect to the detection of structurally damaged houses and buildings, the commission errors are not insignificant. The errors are due to bare ground surface wrongly classified as damaged structures.

Tables 6 summarizes the error or confusion matrix of the morphological approach. The values listed in the table represent the number of pixels correctly and incorrectly identified by the morphological approach as structurally damaged features. The columns in the matrix refer to omission errors whereas the rows refer to commission errors. Producer's and user's accuracies were found to be 52 percent and 82 percent respectively of damaged structures. The overall accuracy achieved was 64 percent. The land-cover types most confused with damaged structures are undamaged man-made features which include paved surfaces and roads, as well as, undamaged houses and buildings.

Discussion and Conclusions

One of the main difficulties with change analysis techniques is the isolation of changes which can be complex and unclear at a glance for various reasons. Shadow formation, and differences in seasonal, sensor and solar conditions at acquisition times can cause false signals or overlap real changes. Another problem with traditional change detection techniques is the reliability of the image registration process

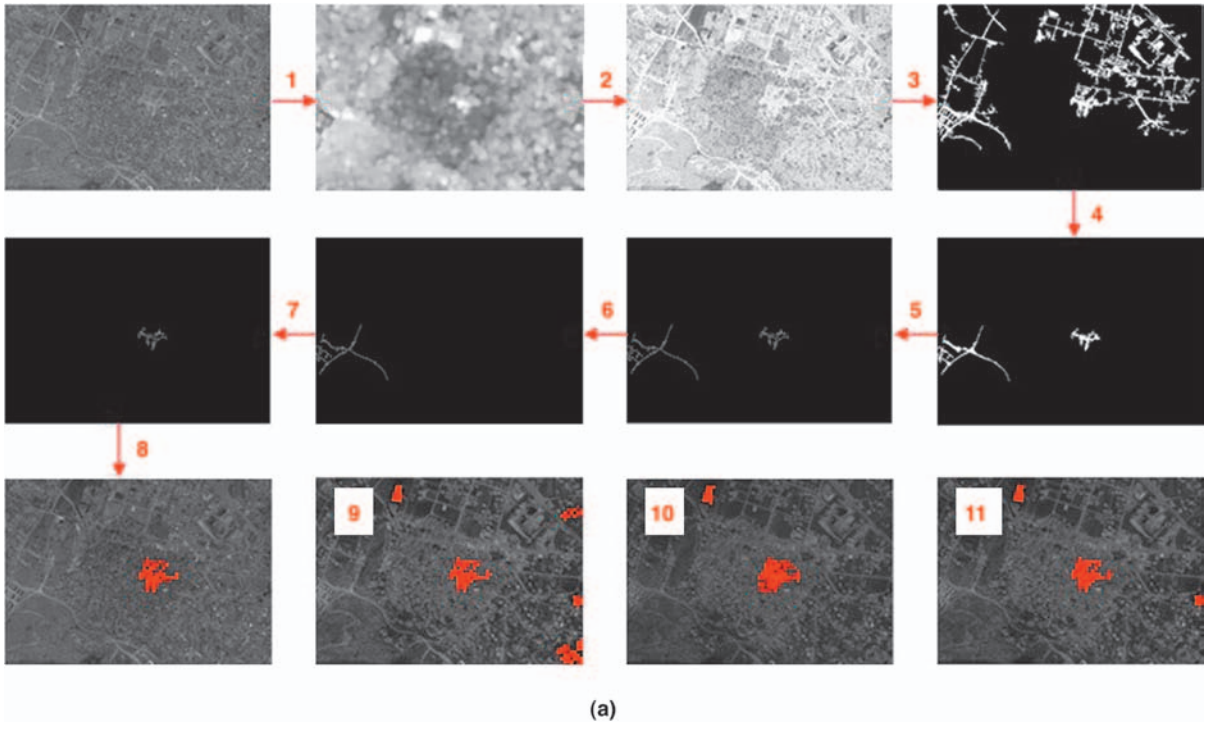

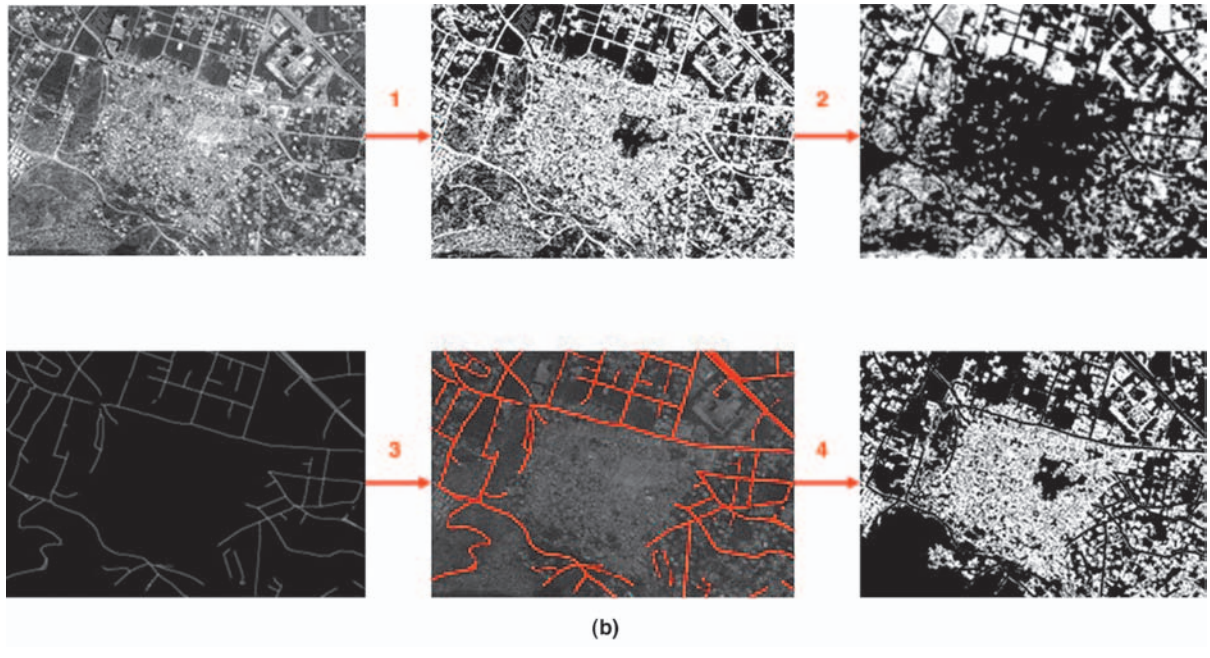

Plate 6. (a) Summary of the Morphological method applied (processing flow shown with arrows) to extract the damaged zone in the Jenin study site. Plate 8a is a zoomed out extent of Plates 1, 3, and 7. Steps 1 through 8 represent processing steps to transform one clip to the next, whereas steps 9 through 11 are outputs: (1) opening of near-infra-red (NIR), or red, or blue or green image; (2) reconstruction by dilation; (3) thresholding using a regional minimus operation; (4) erosion followed by reconstruction by dilation; (5) hit-or-miss transformations; (6) area opening; (7) subtraction; (8) reconstruction by dilation followed by dilation to extract the damage zone from the NIR band; (9) damage zone from the red band; (10) damage zone from the blue band; (11) damage zone from the green band. (b) Summary of the Morphological method applied to extract man-made and vegetation features in the Jenin study site. Plate 6b is a zoomed out extent of Plates 1, 3, and 7. Steps 1 through 4 represent processing steps to transform one clip to the next: (1) white-top-hat followed by thresholding; (2) negating and opening; (3) dilation and intersection of digitised road network with image produced in step 1; (4) subtraction of road network from image produced in step 1.

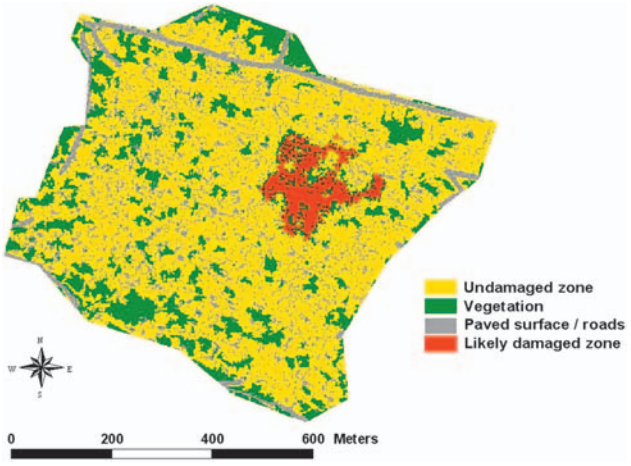

Plate 7. Results of mathematical morphological segmentation and classification of post-conflict image Jenin.

TABLE 5. SUMMARY OF COMMISSION AND OMISSION ERRORS OF TWO METHODS APPLIED IN FYROM (BREST) AND JENIN: OBJECT-ORIENTED CLASSIFICATION USING ECOGNITION OF CHANGE IMAGES AND AUTOMATIC STRUCTURAL DAMAGE CLASSIFICATION WITH ECOGNITION

	Brest		Jenin	
Method	Omission Error (%)	Commission Error (%)	Omission Error (%)	Commission Error (%)
Method type 1. Change Detection:				
(a) Calibrated image difference	12	15	21	24
(b) Non-calibrated image difference	6	22	38	29
(c) Standardised PCA PCs 2&6	12	3	27	24
(d) Non-standardised PCA				
PCs 6&8	19	25	-	-
PCs 2&8	-	-	40	21
Method type 2. Classification of post-conflict image using eCognition	0	24	-	-

TABLE 6. ACCURACY STATISTICS FOR THE MORPHOLOGICAL APPROACH APPLIED TO THE JENIN STUDY SITE. THE CONFUSION MATRIX SHOWS THE NUMBERS OF PIXELS CLASSIFIED AS VEGETATION AND DAMAGED AND UNDAMAGED STRUCTURES IN THE JENIN STUDY SITE

	Reference Data				
Classification Data	Damaged	Vegetation	Undamaged	Row Total	User's Accuracy %
Damaged	3258	25	665	3948	83
Vegetation	994	117	604	1715	7
Undamaged	2001	158	4471	6630	67
Column total	6253	300	5740	12293	100
Producer's accuracy %	52	39	78	100	64*

*Overall classification accuracy.

which is critical when applied to very high-resolution remote sensing images. The results of this research show that supplementing a pixel-based change detection analysis with an object-oriented post-classification, based on the eCognition software, represent an effective approach for interpreting the results of traditional change analysis techniques. Defining different change classes (e.g., vegetation, man-made and other features) facilitates the separation of structurally damaged buildings and houses. The results also show that although the actual boundaries of damaged structures cannot be localized with an adequate accuracy when eCognition is applied both directly to post-conflict satellite images and to change images, eCognition can automatically isolate damaged structures with reasonable accuracy. Similar accuracy results are obtained with the mathematical morphology approach, although determining appropriate segmentation and classification settings are less time consuming than with eCognition.

However, in spite of the sophistication of both types of object-oriented methods and the very high resolution of the satellite images tested in this study, the results show that automatic discrimination of individual features that represent damaged and undamaged houses and/or buildings remains difficult with 1 m to 2 m resolution satellite imagery, and should be further investigated through testing these novel techniques on sub-meter resolution remote sensing data.

The prevailing conclusion is that although eCognition and mathematical morphological techniques are easy to use and versatile; they both require experienced image analysis skills and considerable expenditure of human labour and time exposure to determine the appropriate settings and approaches with respect to segmentation and classification. We conclude that an approach based on a visual comparison of pre- and post-crisis, very high-resolution, remote sensing images remains to be the fastest method for a rapid damage assessment within hours or days of humanitarian crises. However, under less stringent time constraints typifying the reconstruction phase following a disaster, both eCognition and mathematical morphological techniques applied directly to post-disaster, very high-resolution, remote sensing images would be recommended for automatic classification of structural damage maps. Of the two object-oriented methods, mathematical morphology has received less research attention in remote sensing applications of urban areas, particularly in European research studies. This study shows that mathematical morphology is a promising approach that should be further investigated and exploited in remote-sensing based applications supporting humanitarian relief operations.

Acknowledgments

The authors are thankful to Iain Shepherd (JRC) for the acquisition of the satellite images for Brest (FYROM). The authors are also grateful to the three anonymous reviewers for their comments.

References

Acri, 2002, *Georis Software Manual*, ACRI S.A., France, September 2002, 200 p.

Al Khudhairy, D.H.A., I. Caravaggi, and S. Giada, 2003. *Application of change detection analysis and object-oriented classification techniques for structural damage assessment*, Technical Note I.03.66, April, European Communities, Italy, 40 p.

Barnett, V., 1976. The ordering of multi-variate data, *Journal of the Royal Society Statistical Society (A)*, 139(3):318–355.

Bruzzone, L., and S.B. Serpico, 1997. An iterative technique for detection of land-cover transitions in multi-temporal remote

sensing images, *IEEE Transactions on Geoscience and Remote Sensing*, 35(4):858–867.

Bruzzone, L., and D. Prieto, 2000. Automatic analysis of the difference image for unsupervised change detection, TGARS, *IEEE Transactions on Geoscience and Remote Sensing*, 38(3): 1171–1182.

Chandler, D., 2002, What happened in the Jenin refugee camp? URL:http://www.zmag.org//, (last date accessed: 14 February 2005).

Chiroiu, L., G. Andre, and F. Bahoken, 2001. Earthquake loss estimation using high-resolution satellite imagery, GIS Development Net, URL:http://www.gisdevelopment.net/, (last date accessed: 14 February 2005).

Definiens, A.G., 2001. e-Cognition User Guide and documentation, (URL:www.definiens.com, last date accessed: 14 February 2005).

Haala, N., and C. Brenner, 1999. Extraction of buildings and trees in urban environments, *Photogrammetric Engineering & Remote Sensing*, 54 (1):130–137.

Hayes, D.J., and S.A. Sader, 1999. *Change detection techniques for monitoring forest clearing and regrowth in a tropical moist forest*, URL:http://www.ghcc.msfc.nasa.gov/corredor/change_detection.pdf/ (last date accessed: 14 February 2005).

Ingebritsen, S.E., and R.J.P. Lyon, 1985. Principal components analysis of multitemporal image pairs, *International Journal of Remote Sensing*, 6(5):687–696.

International Management Group, 2001. *Damage assessment in the former Yugoslav Republic of Macedonia, Skopje, Macedonia*, Geneva, Switzerland, 153 p.

Kiema, J.B.K., 2002. Texture analysis and data fusion in the extraction of topographic objects from satellite imagery, *International Journal of Remote Sensing*, 23(4):767–776.

Li, X., and A.G.O. Yeh, 1998. Principal component analysis of stacked multi-temporal images for the monitoring of rapid urban expansion in the Pearl River Delta, *International Journal of Remote Sensing*, 19(8):501–1518.

Lunetta, R.S., and C.D. Elvidge, 1998. *Remote Sensing Change Detection*: *Environmental Monitoring Methods and Applications*, Ann Arbor Press, Chelsea, Michigan, USA, 318 p.

Matheron, G., and J. Serra, 2002. The birth of mathematical morphology. In, *Proceedings of VIth International Symposium on Mathematical Morphology, Sydney, Australia,* 2002 (H. Talbot and R. Beare, editors), Commonwealth Scientific and Industrial Research Organisation, pp. 1–16, URL:www.cmis.csiro.au/ismm2002/proceedings/PDF/00_matheron.pdf, (last date accessed: 14 February 2005).

Matsouka, M., and F. Yamazaki, 2002. Application of the damage detection method using SAR intensity images to recent earthquakes, *Proceedings of the IGARSS 2002, International geoscience and remote sensing symposium, Remote sensing: integrating our view of the planet*, Toronto, Canada, IV: 2042–2044.

Matsouka, M., and F. Yamazaki, 2003. Application of a methodology for detection of building- damage area to recent earthquakes using SAR intensity imageries and its validation, *Proceedings of the 7th EERI U.S.-Japan Conference on Urban Earthquake Hazard Reduction,* Maui, pp. 310–315, *URL*:http://www.eeri.org/news/meetings/7usjpw/EERI-Notebook.pdf, (last date accessed: 14 February 2005).

Mitomi, H., F. Yamazaki, and M. Matsuoka, 2002. Application of automated damage detection of buildings due to earthquakes by panchromatic aerial television images, *Proceedings of the 7th U.S. National Conference on Earthquake Engineering*, 21–25 July, Boston, Massachusetts, USA, unpaginated CD-ROM.

Mücher, C.A., K.T. Steinnocher, F.P. Kressler, and C. Heunks, 2000. Land cover characterization and change detection for environmental monitoring of pan-Europe, *International Journal of Remote Sensing*, 21(6&7):1159–1181.

Nielsen, A., K. Conradsen, and J. Simpson, 1998. Multivariate alteration detection (MAD) and MAP post processing in multispectral bitemporal image data: new approaches to change detection studies, *Remote Sensing of Environment*, 64:1–19.

Niemeyer, I., and M. J. Canty, 2001. Object-oriented post-classification of change images, *Proceedings of SPIE's International Symposium on Remote Sensing*, Toulouse, France, 17–21 September, Vol. 4545.

Research Systems, Inc., 1999. *ENVI User's Guide*, Research Systems, Inc., July, 864 p.

Saito, K., and R.J. Spence, in Press. Using high-resolution satellite images for post-earthquake building damage assessment: a study following the 26.1.01 Gujarat earthquake, *Earthquake Spectra*.

SDC Information Systems, 2001. *SDC Morphology toolbox for Matlab 5 user's guide*, Naperville, Illinois, USA, 303 p.

Soille, P., 1996. Morphological partitioning of multi-spectral images, *Journal of Electronic Imaging*, 5(3):252–265.

Soille, P., and M. Pesaresi, 2002. Advances in mathematical morphology applied to geoscience and remote sensing, *IEEE Transactions on Geoscience and Remote Sensing*, 30(5):1054–1060.

Soille, P., 2003. *Morphological Image Analysis: Principles and Applications*, Springer-Verlag Berlin, Germany, 391 p.

Stow, D., D. Chen, and L. Coulter, 2001. Detection of pixel-level land-cover changes with multi-temporal imagery: Theory and examples with imagery of 1 meter and 1 kilometer spatial resolutions, *Proceedings of the First International Workshop on the Analysis of Multi-Temporal Remote Sensing Images*, University of Trento, Italy, 13–14 September.

United Nations, 2002. Jenin Report of the Secretary General Prepared Pursuant to General Assembly Resolution ES-10/10, URL:http://www.un.org/, (last date accessed: 14 February 2005).

Zhang, Y., 1999. Optimisation of building detection in satellite images by combining multi-spectral classification and texture filtering, *Journal of Photogrammetry and Remote Sensing*, 50:50–60.

(Received 20 November 2003; accepted 23 January 2004; revised 08 March 2004)